The nature of electron acceptor (MnIV/NO3) triggers differential expression of genes associated with stress and ammonium limitation responses in Shewanella algae C6G3

Axel Aigle, Patricia Bonin, Nicolas Fernandez -Nunez, Béatrice B. Loriod, Sophie Guasco, Aurélie Bergon, Fabrice Armougom, Chantal Iobbi-Nivol, Jean Imbert, Valerie Michotey

▶ **To cite this version:**

2   **The nature of electron acceptor (MnIV/NO3) triggers differential expression of genes associated**

3   **with stress and ammonium limitation responses in *Shewanella algae* C6G3**

4

5   Axel Aigle[1], Patricia Bonin[1], Nicolas Fernandez -Nunez[2], Béatrice Loriod[2], Sophie Guasco[1], Aurélie

6   Bergon[2], Fabrice Armougom[1], Chantal Iobbi-Nivol[3], Jean Imbert[2], Valérie Michotey*[1].

7

8   [1]Aix Marseille Univ, Univ Toulon, CNRS, IRD, MIO UM 110, Mediterranean Institute of

9   Oceanography, Marseille, France

10   [2] UMR_S 1090, TGML/TAGC, Aix-Marseille Université, Marseille F-13009, France

11   [3] Aix-Marseille Université, CNRS, BIP Bioénergétique et Ingénierie des Protéines UMR 7281, 13402,

12   Marseille, France

13   **Abstract-**

14   *Shewanella algae* C6G3 can reduce dissimilatively nitrate into ammonium and manganese-oxide

15   (MnIV) into MnII. It has the unusual ability to produce anaerobically nitrite from ammonium in the

16   presence of MnIV. To gain insight into their metabolic capabilities, global mRNA expression patterns

17   were investigated by RNA-seq and qRT-PCR in cells growing with lactate and ammonium as carbon

18   and nitrogen sources and with either MnIV or nitrate as electron acceptors. Gene exhibiting higher

19   expression levels in the presence of MnIV belonged to functional categories of carbohydrate, coenzyme,

20   lipid metabolisms and inorganic ion transport. Comparative transcriptomic pattern between MnIV and

21   NO_3 revealed that the strain presented an ammonium limitation status with MnIV, despite the presence

22   of non-limiting concentration of ammonium under both culture conditions. In addition, in presence of

23   MnIV, *ntrB/nrtC* regulators, ammonium channel, nitrogen regulatory protein P-II, glutamine synthetase

24   and asparagine synthetase glutamine dependent genes were over-represented. Under nitrate condition,

25   the expression of genes involved in the synthesis of several amino acids was increased. Finally,

26   expression level of genes associated with the general stress response was also amplified and among

27   them, *katE,* a putative catalase/peroxidase present on several *Shewanella* genomes, was highly expressed

28   with a relative median value higher in MnIV condition.

29

30   *Key words: Shewanella algae, Manganese-oxide, nitrate, nitrogen-limitation, transcriptome, catalase*

31   *Corresponding author: Valerie Michotey, Marine Institute of Oceanography, M.I.O, campus de
32   Luminy, batiment Oceanomed. 13288 Marseille, France
33   Tel:00330486090555; Valerie.michotey@univ-amu.fr
34

35

1. Introduction

The genus *Shewanella* widely distributed in marine and freshwater environments is recognized for its metabolic versatility toward broad range of electron acceptors, including oxygen (O_2), nitrate (NO_3^-), nitrite (NO_2^-), fumarate, ferric iron, manganese-oxide (MnO_2 or MnIV), thiosulfate, elemental sulfur, trimethylamine N-oxide (TMAO), dimethyl sulfoxide (DMSO), and anthraquinone-2,6-disulfonate (AQDS) (Beliaev *et al.*, 2005, Fredrickson *et al.*, 2008). This metabolic versatility provides high competitiveness to these species, especially in stratified environments with electron acceptor gradients. The marine sediments are examples where dissolved oxygen concentration decreases with depth following a vertical slope. Oxygen is substituted by alternative electron acceptors leading to their vertical zonation comprising from surface to deep, $NO_{2/3}^-$, Mn(III/IV), Fe(III), SO_4^{2-}, CO_2^- (Emerson & Hedges, 2006, Hansel, 2017). The metabolic versatility of *Shewanella* species confers them an important role in the turnover of organic matter and in the carbon cycle, coupled to anaerobic respiration with electron acceptors, such as FeIII, MnIV and $NO_{2/3}^-$ (Coates *et al.*, 1998).

In marine sediments, the concentration of ammonium is generally much higher than that of $NO_{2/3}$. These nitrogen oxyanions are mainly produced from ammonium by nitrification in the overlying aerobic zone and can diffuse to the anaerobic area where they fuel many dissimilatory reduction pathways (e. g. denitrification, dissimilatory reduction of nitrate into ammonium or Anammox) leading or not to a nitrogen lost for the system such as gaseous production (Bonin *et al.*, 1998). Many studies have highlighted the strong coupling between aerobic ammonium oxidation and anaerobic NO_3^- or NO_2^- reduction communities (Fernandes *et al.*, 2016). The study of organisms and mechanisms leading to $NO_{2/3}^-$ production is therefore essential for the comprehension of the functioning of the anaerobic part of sediments. Several studies have demonstrated the stimulation of activities associated with nitrogen cycle in anaerobic marine sediments in the presence of MnIV, supporting the hypothesis of the occurrence of a manganese-oxide (MnIV) dependent anaerobic $NO_{2/3}^-$ production pattern (Luther *et al.*, 1997, Anschutz *et al.*, 2005, Javanaud *et al.*, 2011, Fernandes *et al.*, 2015). The anaerobic ammonium oxidation seems to be favored with a 2-4 fold NH_4/MnIV concentration ratio and is concomitant to higher ammonium consumption (Lin & Taillefert, 2014).

During the analysis of the anaerobic $NO_{2/3}^-$ peak observed in some marine sediments, a *Shewanella algae* C6G3 strain was isolated and characterized from an intertidal zone (Javanaud et al., 2011, Aigle et al., 2015, Aigle et al., 2017). *S. algae* is an ubiquitous species of coastal marine environments (Caccavo *et al.*, 1992, Beleneva *et al.*, 2009) and the strain C6G3 can perform the dissimilatory reduction of nitrate into ammonium and MnIV reduction. It displays the additional ability to produce anaerobically biotic NO_2^- with ammonium as the sole nitrogen source and MnIV as the sole

electron acceptor. Neither ammonia monooxygenase nor hydroxylamine oxidase gene, known in aerobic nitrifiers for oxidation of ammonium into nitrite or nitrate were detected within C6G3 genome (Aigle et al., 2017). In addition, no genes were identified coding for either hydrazine synthase, hydrazine dehydrogenase or hydroxylamine oxidase involved in Anammox in which ammonium is used as electron donor and nitrite as electron acceptor in anaerobiosis and generating N_2. Among the genus *Shewanella*, many studies have focused on the *S. oneidensis* MR-1, the most-described strain capable of dissimilatory metabolism of MnIV. The mechanism of extracellular electron exchange has been particularly well detailed (Richardson *et al.*, 2012, Shi *et al.*, 2012, White *et al.*, 2016). Using microarrays, specific expression profiles have been determined after short time incubations with individual non-metal electron acceptors resulting in the identification of unique groups of nitrate-, thiosulfate- and TMAO-induced genes (Beliaev *et al.*, 2005).

Several differences between *S. algae* C6G3 and *S. oneidenis* genomes have been characterized so far, especially concerning N-cycle and MnIV reduction. Indeed, in *S. algae*, additional genes are present such as a second *nap* operon (encoding a nitrate reductase), *nrfA* (encoding a second nitrite reductase) and additional genes in the MTR pathway (*mtrH*) (Aigle et al., 2017). Furthermore, in contrast to *S. algae* C6G3 and ATCC5119 strains, no anaerobic biotic $NO_{2/3}$ production was detected in *S. oneidensis* with ammonium as the sole nitrogen source and MnIV as the sole electron acceptor (Aigle et al., 2017). To understand the impact of MnIV and NO_3^- on the metabolism of *S. algae C6G3,* transcriptomic profiles obtained in the presence of these electron acceptors were compared. Several putative overexpressed pathways were further investigated along growth by qRT-PCR. Due to the capability of the strain to oxidize ammonium in nitrite in anaerobiosis, these analyses were focused on NH_4 metabolism and stress response.

Materials and Methods

Growth conditions

Shewanella algae C6G3 was grown anaerobically at 28 °C in artificial sea water (Baumann *et al.*, 1971) with DL-lactate (25 mM), K_2HPO_4 (0.43 mM), $FeSO_4$ (13,2 µM), NH_4Cl (20 mM) and trace mineral element solution and vitamin (Balch *et al.*, 1979). Nitrate (3 mM) or manganese oxides (1 mM) were added as sole source of electron acceptor. Manganese oxide was synthesized following the protocol of Laha (Laha & Luthy, 1990). Cells were grown under strict anaerobic conditions with a 100% N_2 gas head space. Cultures dedicated to RNA-seq, expression profiling, or physiology were made in duplicate. Nitrate, nitrite, MnII and 16S rDNA were measured as previously described (Aigle et al., 2017)

Transcriptome analysis

For RNA-seq, cells from two independent cultures for each growth condition at three quarters of their exponential phase of growth were pelleted and washed twice with RNAprotect® Bacteria Reagent (Qiagen): Tris-NaCl buffer (0.05 M Tris; 0.15 M NaCl; pH 7.8) 2:1 and rinsed with Tris-NaCl buffer. After lysis in RLT buffer of RNeasy® kit (Qiagen), total RNA was extracted with phenol: chloroform: isoamyl alcohol 125:24:1 pH 4.5, gently mixed and centrifuged 15 min at 12.000 g at 4 °C, and then with chloroform: isoamyl alcohol 24:1, gently mixed and centrifuged 15 min at 12.000 g at 4 °C. Total RNA samples were purified using RNeasy® Mini QIAcube Kit (Qiagen) and DNA contamination was removed using the TURBO DNA-free^{TM} kit (Ambion® by Life Technologies^{TM}) according to the manufacturer's instructions.

After RNA quality check, (Agilent 2100 Bioanalyzer Santa Clara, CA, USA) and quantification (Nanodrop 2000c Thermo Scientific), the absence of DNA contamination was verified by PCR following the protocol of Aigle *et al.* (2017). The Transcriptomic and Genomic Marseille-Luminy (TGML) platform performed further sample treatments (Amrani *et al.*, 2014). Templates sequencing was performed with semiconductor sequencing chips 318 on the Ion Torrent PGM (Life Technology). Despite the lower number of reads generated by this technology, it was chosen because at that time it allowed to sequence longer reads than Illumina. The RNA-seq data performed in duplicated for each culture condition have been deposited on NCBI GEO platform (accession number GSE109146).

RNA data were analyzed as previously described (Amrani *et al.*, 2014). Briefly, the R package DESeq was used to analyze the differential expression of genes between the different culture conditions (Anders & Huber, 2010). P-values were calculated and adjusted for multiple testing using the false discovery rate controlling procedure (Benjamini & Hochberg, 1995). An adjusted P-value <0.05 was considered statistically significant. The Kegg Orthology identifiers of genes and the KEGG pathways assignment were performed on *S. algae* C6G3 genome using KAAS tool (KEGG Automatic Annotation Server, GenomeNet).

For the kinetic of gene expression, RNA was extracted along growth (4 or 5 time points spread from early exponential to early stationary phase of growth) from two independent cultures for each growth condition. Reverse transcriptase reactions with random primers, cDNA quantification by qPCR and data analysis were performed as previously described (Aigle *et al.*, 2017). Primers used for qPCR are listed in Table S1. Row data of target gene expression per ng of total RNA are presented in Table S2. Two technical qPCR quantifications were performed for each RNA extraction. From a previous study, we

5

134 have noticed a lower quality of RNA from MnIV grown cells due to splitting of RNA by MnII. The

135 quantification of the expression of the house-keeping gene (*rpoD*) encoding the sigma^{70} subunit of the

136 RNA polymerase was used to normalize gene expression in order to avoid putative bias from RNA

137 extraction and reverse transcription efficiency. The median value for *rpoD*/ng of total RNA from

138 duplicate MnIV or NO_3 grown cells at all the time points were $1.49 . 10^3$ and $5.47\ 10^3$ cDNA/ng RNA,

139 respectively. No clear tendency was seen according to either condition or phase of growth (Fig S1). All

140 cDNA quantifications by qPCR were done on the same reverse transcription.

141

Results and discussion

143 RNA-seq assays generated 1,725,084 high-quality reads for the four tested samples (two per culture

144 conditions). Between 83 to 95% of the high-quality reads were mapped to *S. algae* C6G3 genome (Table

145 S3). Correlation matrix between RNA-seq normalized expression levels of each independent culture

146 obtained with DESeq (Anders & Huber, 2010) indicated that the similarity between the 2 biological

147 replicates was above 90% (Fig.S2).

148 This preliminary study allowed to identify 148 genes as differentially expressed (adjusted p-value

149 <0.05), 67 and 81 were over-represented under MnIV or nitrate conditions, respectively (Fig S3, S4,

150 Table S4). Most of significant differentially expressed genes belonged to COG categories of energy

151 production and conversion (C), amino acid transport and metabolism (E), carbohydrate transport and

152 metabolism (G) , co-enzyme metabolism (I), lipid metabolism (L), inorganic ion transport and

153 metabolism (P), posttranslational modification, protein turnover and chaperones (O) (Fig. 1).

154 Under both growth conditions, lactate was the only carbon source available and was partially oxidized

155 into acetate that accumulated in the medium as for many species of its genus (Fig. 2) (Aigle *et al.*, 2015)

156 (Tang *et al.*, 2007, Lian *et al.*, 2016). *S. algae* C6G3 genome contains five formate dehydrogenase gene

157 clusters (Aigle *et al.*, 2015),among them four, i.e. *fdnGHI-fdhC, fdhA1B1C1, fdhA2B2C2, hyaAB,* are

158 also present in *S. oneidensis* MR-1, while the fifth, i.e. *fdoGHI* is present in *E. coli* and in *Sinorhizobium*

159 *meliloti* (Heidelberg et al., 2002, Wang & Gunsalus, 2003, Pickering & Oresnik, 2008). Under nitrate

160 condition, two formate dehydrogenase clusters (*fdnGHI-fdhD* and *fdoGHI* gene clusters) were over-

161 represented in RNA seq compared to MnIV condition (log2 fold change MnIV/NO_3 between -3.7 and -

162 6.1; and -3.6 and 5.6, respectively Table S4)). Regulation of *fdnGHI* genes by nitrate was previously

163 demonstrated in *E. coli* (Wang & Gunsalus, 2003) and *S. oneidensis* MR-1 (Beliaev *et al.*, 2005) whereas

164 *fdoGHI* was *shown* to encode a formate dehydrogenase complex NAD^+ independent (Pickering &

165 Oresnik, 2008). Considering its over-representation under nitrate condition observed in our study,

166 *fdoGHI* is probably implicated in the process of nitrate reduction. The *fdh* gene cluster was over-

represented in the presence of MnIV (genes *fdhA* and *fdhC*, log2 fold change MnIV/NO3 between 1.7 and 2.33, Table S4). Under this growth condition, it has been proposed that nitrate and nitrite are produced from ammonium (Aigle et al 2017 and Fig.2). Consequently, the dehydrogenase encoded by the *fdh* cluster could be involved in the process of either $NO_{2/3}^-$ production or MnIV reduction.

Nitrate and nitrite reduction is a stepwise process during *S. algae* C6G3 anaerobic growth with nitrate as electron acceptor (Fig. 2). Dissimilatory nitrate reduction into ammonium is catalyzed by two enzymes, the nitrate reductase (*napA*) oxidizing nitrate to nitrite, and the nitrite reductase formate dehydrogenase (*nrfA*) that oxidizes nitrite to ammonium (Simon, 2002, Simpson *et al.*, 2010, Aigle *et al.*, 2015). As the RNA-seq was performed at the ¾ of the exponential phase of growth when all nitrate is reduced to nitrite, an over-representation of the *nrfA* gene in RNA seq was expected (log2 fold change MnIV/NO3 of -2.5, Table S4) in agreement with our previous results obtained by qRT-PCR (Aigle et al., 2017). The similar expression level of the metal transfer reduction operon (*mtrABCDEF*) between both growth conditions is also in agreement with previous observations (Beliaev *et al.*, 2005, Aigle *et al.*, 2017).

The over-representation in RNA seq of genes responsible for ammonium assimilation under N-limiting condition, when MnIV was the electron acceptor, is the most striking observation of the present study (Fig. 3, Table S4). In liquid medium, ammonium (NH_4^+) concentration is in equilibrium with ammonia (NH_3) according to acid base equilibrium constant (Ka). Regardless the electron acceptor, the culture medium contained at the beginning of the growth 20 mM of NH_4Cl. According to the pKa of NH_4^+/NH_3 (9.23) and the pH of the medium (7.8), the NH_3 concentration is estimated at ~1.2 mM. While ammonia gas can passively diffuse through the cellular membrane, NH_4^+ needs to be absorbed through an ammonium channel encoded by the *amtB* gene. This gene is expressed only under drastic ammonium limitation (van Heeswijk *et al.*, 2013). In this study, despite NH_4^+/NH_3 availability in the cultures, the NH_4^+ uptake pathway genes were over-represented in the presence of MnIV compared to that of nitrate. Moreover, genes coding for the NRI/NRII-two component system nitrogen regulator (*ntrB/nrtC* also called *glnG/glnL,* log2 fold change MnIV/NO3 of 2.9 and 3.5*)*, the ammonium channel (*amtB,* log2 fold change MnIV/NO3 of 6.1), the nitrogen regulatory protein P-II (*glnK,* log2 fold change MnIV/NO3 of 5.5), the glutamine synthetase (*glnA,* log2 fold change MnIV/NO3 of 2.7) and the asparagine synthetase glutamine dependent (*asnB,* log2 fold change MnIV/NO3 of 6.5) were over-represented similarly (Table S4). Entry of ammonium has been convincingly shown to occur through ammonium channels that are blocked by the nitrogen regulatory protein P-II, encoded by the *glnK* gene. The association of AmtB/PII complex is controlled by the UTase enzyme, sensitive to the glutamine product of the glutamine

synthetase encoded by the *glnA*, to 2-oxoglutarate concentration (an intermediate of the Krebs cycle and an indicator of nitrogen status) and to MgII and ADP/ATP ratio (van Heeswijk *et al.*, 2013*)*.

Under nitrogen limitation, GlnA catalyzes the formation of glutamine from glutamate and ammonia. The produced glutamine is the substrate of glutamate synthase (GOGAT), which catalyzes the conversion of 2-oxoglutarate and glutamine into two molecules of glutamate. In order to maintain balanced metabolism, the cell must coordinate the assimilation of nitrogen with the assimilation of carbon and other essential nutrients. This coordination is carried out in part by a signal transduction system, which measures signals of carbon and nitrogen status and regulates the activity of GlnA, and by the transcription of nitrogen-regulated (Ntr) genes, whose products facilitate the use of poor nitrogen sources (van Heeswijk *et al.*, 2013).

S. algae C6G3 genes organization is similar to what is known for *E. coli where glnA* is part of the *glnALG* or *glna-ntrBC* operon whereas *amtB* and *glnK* are located in close vicinity (data not shown). The kinetic of the expression of these two operons was followed by qRT-PCR targeting one of their genes (*glnA* and *amtB*) at 4 or 5 time points in duplicate-cultures with MnIV or NO_3 as electron acceptors. The median value of *glnA* expression level of all time points of both duplicate cultures was higher under MnIV than under NO_3 condition, whether it is expressed in absolute quantification (5.98 10^4 vs 0.89 10^4 of *glnA* cDNA/ng RNA, Table S2) or relative to *rpoD* (46.1 vs 2.9). This over-expression was observed for all time points of the cultures confirming our RNA-seq results (Fig. 3). The *rpoD*-relative expression level of *amtB* was lower than that of *glnA* but presented also a higher median under MnIV (1.7) than under nitrate (0.6) conditions. Its expression in both culture duplicates was higher under MnIV condition than under NO_3 for three of the four time points of the cultures (Fig. 3). Since the expression of these two genes is induced by low intracellular NH_3/NH_4^+ concentration, this observation suggests that this strain senses nitrogen limitation in the presence of MnIV throughout growth. It is known that 2-oxoglutarate can stimulate ammonium assimilation by dissociation of the Amt-GlnK complex (van Heeswijk *et al.*, 2013). Interestingly, the increased expression of the gene coding for isocitrate deshydrogenase (IDH), leading to 2-oxoglutarate production, was also confirmed by qRT-PCR in the early exponential phase of growth suggesting a probable production of 2-oxoglutarate, preventing the closure of ammonium channel in the presence of MnIV (Fig.3).

Several explanations could be proposed for the surprising difference of nitrogen status (limiting *vs* non-limiting available nitrogen) between cultures grown with either nitrate or MnIV as electron acceptors. The limitation by the initial concentration of ammonium concentration (20 mM) can be excluded since its concentration was identical in both culture media and the overexpression of *glnA* and *amtB* occurred from the early exponential phase of growth. Furthermore, several genes responsible for amino acid synthesis such as valine/isoleucine (*ilvC*), methionine /threonine (*metB*) or cysteine (*cysK* and *cysN*)

were under-expressed under MnIV condition (Fig. 3). The ammonium need for the general biomass development is probably much lower in presence of MnIV since the cell density at the end of the culture was 28 fold lower than that obtained with nitrate. (Fig.2). Ammonium could be destined to anabolism of specific compounds as suggested by the synthesis of higher number of cytochromes coupled to the overproduction of some of them in MnIV grown cells (Fig. S4) and by the overexpression of genes included in carbohydrate, inorganic ion transport and metabolism; coenzyme and lipid, metabolism COG categories (Fig.1). Among these categories, seven genes involved in the synthesis of storage products such as glycogen were found (*glgA*, *glgB*, *glgC*, *glgP*,*pgl*, *malQ*, log2 fold change MnIV/NO_3 between 2.4 and 5.5, Table S4). The expression of one of them, *glgB* was confirmed by qRT-PCR for two time points of growth under MnIV condition (Fig. 3). Glycogen has been shown to accumulate in large amount within cells when growth is limited by a deficiency of some factors other than the carbon and energy source (Wilkinson, 1963). Other hypotheses could be formulated to explain the expression of genes induced by NH_3/NH_4^+ limitation: (i), an abiotic reaction involving Mn(II) and scavenging part of available ammonia such as $Mn^{2+} + 2NH_3 + 2H_2O \leftrightarrow Mn(OH)_2 + 2NH_4^+$; (ii) an additional need of ammonium to partially scavenge the oxides generated from MnIV ($MnO2$) reduction into MnII, concomitant to nitrite formation with an unresolved mechanism. Nitrite consumption is visible between 20 and 40 h in culture grown with MnIV (Fig.2). Due to the presence of *nrfA* on *S. algae* genome and its expression under this condition (Aigle *et al.*, 2017), the formed nitrite could be further reduced by DNRA into ammonium; (iii) the last one could be the combination of several causes. Further investigations are needed to validate one or several of these hypotheses.

Nitrate (NO_3) dissimilation may produce reactive oxygen/nitrogen species (RONS). For example, *E. coli* cells, grown anaerobically with nitrate as terminal electron acceptor, generate significant NO on adding nitrite. The periplasmic cytochrome *c* nitrite reductase (Nrf) was shown, by comparing Nrf$^+$ and Nrf$^-$ mutants, to be largely responsible for NO generation (Corker & Poole, 2003). From micro-array, upregulation of a large number of stress responses genes under both nitrate and metal-reducing conditions have been shown in *S. oneidensis* (Beliaev *et al.*, 2005). In *S. algae* C6G3, several genes of stress responses were expressed similarly under nitrate compared to MnIV condition, indicating an analogous stress status. However several other genes (*clpA, clpB*, *katE*, *groEL*, *dnaK*, *rpoS, katE,* Fig.2 and Table S4) known to be involved in the general stress response, are apparently over-represented at least in one conditions as suggested by our RNA-seq preliminary results. The time course of their expressions along growth were investigated by qRT-PCR. Overall, the median expression levels of genes *dnaK*, *groEL* encoding chaperones*, rpoS* encoding the general stress response sigma factor*,* and *clpB* encoding a protease machinery component were higher under nitrate than MnIV condition whether they were expressed either as absolute quantification (*dnaK* mRNA abundance *:* 5.68 10^4 vs 3.08 10^3 cDNA/ng RNA; *groEL* mRNA abundance: 7.8 10^3 vs 2.93 10^3 cDNA/ng RNA; *rpoS* mRNA abundance:

269   2.77×10^4 vs 3.07×10^3 cDNA/ng RNA; *clpB* mRNA abundance: 3.89×10^3 vs 5.16×10^2 cDNA/ng RNA,

270   Table S 2), or relative to *rpoD* (*dnaK:4.3 vs 2.5*; *groEL*: 1.5 vs 1.12; *rpoS* : 5.4 vs 2.1, *clpB :* 0.38 vs

271   0.31). However, their temporal expressions differed. Considering *rpoS*, its relative expression level was

272   higher in the presence of nitrate than of MnIV for all the phases of growth (early expo 2, exp, early stat

273   1, Fig.4). In contrast, the expression of *dnaK*, *clpB* and *groEL* depended on the phase and was

274   overexpressed under MnIV condition in early exponential phase of growth whereas an opposite tendency

275   was seen under NO_3 condition in exponential phase of growth concomitant with the nitrite peak (Fig. 2,

276   4).

277   Interestingly, under manganese condition, *S. algae* C6G3 transcriptome analysis underlined the strong

278   over-representation (log2 fold change of 4.7, Table S3) of one out of the four catalase/peroxidase genes

279   present in its genome (SA002_03500, corresponding to *KatE* found in several *Shewanella* species, Table

280   S5). Among the stress genes identified by RNA-seq, *katE* relative expression level was higher

281   particularly under MnIV condition, as shown by the median *rpoD*-relative expression of *katE* reaching

282   21.3 and 6.7 under MnIV or NO_3 conditions, respectively. At a lesser extent, the preferential expression

283   under MnIV condition presented the same tendency for the absolute quantification (*katE* mRNA

284   abundance 3.41×10^4 vs 3.36×10^4 cDNA/ng RNA). The over-representation of *katE* in the presence of

285   MnIV was confirmed by qRT-PCR in early exponential and stationary phase of growth (Fig. 4),

286   suggesting a specific response to MnIV or to a metabolic byproduct of the strain under these growth

287   conditions.

288   **4. Conclusion**

289   Our aim was to better understand the metabolism of *S. algae* when it encounters different electron

290   acceptors such as MnIV and nitrate and the strategies the bacterium develops to adapt its energetic

291   pathways. A transcriptomic analysis revealed major differences in the expression of genes involved in

292   central metabolism such as amino acid synthesis and ammonium assimilation linked to the use of

293   different electron acceptors. Furthermore, *katE*, a gene encoding for a putative catalase/peroxidase, was

294   highly expressed in both conditions but with a greater relative median value under MnIV condition

295   suggesting an important role.

296

300

301

References

Aigle A, Michotey V & Bonin P (2015) Draft-genome sequence of Shewanella algae strain C6G3. *Stand Genomic Sci* **10**.

Aigle A, Bonin P, Iobbi-Nivol C, Mejean V & Michotey V (2017) Physiological and transcriptional approaches reveal connection between nitrogen and manganese cycles in Shewanella algae C6G3. *Scientific Reports* **7**: 44725.

Amrani A, Bergon A, Holota H, Tamburini C, Garel M, Ollivier B, Imbert J, Dolla A & Pradel N (2014) Transcriptomics reveal several gene expression patterns in the piezophile Desulfovibrio hydrothermalis in response to hydrostatic pressure. *PLoS One* **9**: e106831.

Anders S & Huber W (2010) Differential expression analysis for sequence count data. *Genome Biol* **11**: R106.

Anschutz P, Dedieu K, Desmazes F & Chaillou G (2005) Speciation, oxidation state, and reactivity of particulate manganese in marine sediments. *Chem Geol* **218**: 265-279.

Balch WE, Fox GE, Magrum LJ, Woese CR & Wolfe RS (1979) Methanogens - Re-Evaluation of a Unique Biological Group. *Microbiol Rev* **43**: 260-296.

Baumann P, Baumann L & Mandel M (1971) Taxonomy of marine bacteria: the genus Beneckea. *J Bacteriol* **107**: 268–294.

Beleneva IA, Magarlamov TY, Eliseikina MG & Zhukova NV (2009) Biochemical and pathogenic properties of the natural isolate of Shewanella algae from Peter the great bay, sea of Japan. *J Invertebr Pathol* **102**: 250-255.

Beliaev AS, Klingeman DM, Klappenbach JA, Wu L, Romine MF, Tiedje JM, Nealson KH, Fredrickson JK & Zhou J (2005) Global transcriptome analysis of Shewanella oneidensis MR-1 exposed to different terminal electron acceptors. *J Bacteriol* **187**: 7138-7145.

Benjamini Y & Hochberg Y (1995) Controlling the false discovery rate-a practical and powerfull approach to multiple testing. *J Roy Stat Soc B Met* **57**: 289-300.

Bonin P, Omnes P & Chalamet A (1998) Simultaneous occurence of denitrification and nitrate ammonification in sediments of the french mediterranean coast. *Hydrobiologia* **389**: 169-182.

Caccavo F, Blakemore RP & Lovley DR (1992) Isolation and characterisation of a FE(III)-reducing and Mn(IV)-reducing microorganisms from Great Bay, New Hampshire. *Abstr Pap Am Chem S* **203**: 1236GEOC.

Coates JD, Councell T, Ellis DJ & Lovley DR (1998) Carbohydrate oxidation coupled to Fe(III) reduction, a novel form of anaerobic metabolism. *Anaerobe* **4**: 277-282.

Corker H & Poole RK (2003) Nitric oxide formation by Escherichia coli. Dependence on nitrite reductase, the NO-sensing regulator Fnr, and flavohemoglobin Hmp. *J Biol Chem* **278**: 31584-31592.

Emerson S & Hedges J (2006) *6.11 Sediment Diagenesis and Benthic Flux*. Elsevier, Netherlands.

Fernandes SO, Javanaud C, Michotey VD, Guasco S, Anschutz P & Bonin P (2016) Coupling of bacterial nitrification with denitrification and anammox supports N removal in intertidal sediments (Arcachon Bay, France). *Estuar Coast Shelf S* **179**: 39-50.

Fernandes SO, Javanaud C, Aigle A, Michotey VD, Guasco S, Deborde J, Deflandre B, Anschutz P & Bonin PC (2015) Anaerobic nitrification–denitrification mediated by Mn-oxides in meso-tidal sediments: Implications for N2 and N2O production. *Journal of Marine Systems* **144**: 1-8.

Fredrickson JK, Romine MF, Beliaev AS, *et al.* (2008) Towards environmental systems biology of Shewanella. *Nat Rev Microbiol* **6**: 592-603.

Hansel CM (2017) Manganese in Marine Microbiology. *Adv Microb Physiol* **70**: 37-83.

Heidelberg JF, Paulsen IT, Nelson KE, *et al.* (2002) Genome sequence of the dissimilatory metal ion-reducing bacterium Shewanella oneidensis. *Nat Biotechnol* **20**: 1118-1123.

Javanaud C, Michotey V, Guasco S, Garcia N, Anschutz P, Canton M & Bonin P (2011) Anaerobic ammonium oxidation mediated by Mn-oxides: from sediment to strain level. *Res Microbiol* **162**: 848-857.

Laha S & Luthy RG (1990) Oxidation of aniline and otherprimary aromatic-aminesby Manganes-dioxide. *Environ Sci Technol* **24**: 363-373.

Lian Y, Yang Y, Guo J, Wang Y, Li X, Fang Y, Gan L & Xu M (2016) Electron acceptor redox potential globally regulates transcriptomic profiling in Shewanella decolorationis S12. *Sci Rep* **6**: 31143.

Lin H & Taillefert M (2014) Key geochemical factors regulating Mn(IV)-catalyzed anaerobic nitrification in coastal marine sediments. *Geochim Cosmochim Ac* **133**: 17-33.

Luther GW, Sundby B, Lewis BL, Brendel PJ & Silverberg N (1997) Interactions of manganese with the nitrogen cycle: Alternative pathways to dinitrogen. *Geochimica Et Cosmochimica Acta* **61**: 4043-4052.

Pickering BS & Oresnik IJ (2008) Formate-dependent autotrophic growth in Sinorhizobium meliloti. *J Bacteriol* **190**: 6409-6418.

357   Richardson DJ, Butt JN, Fredrickson JK*, et al.* (2012) The 'porin-cytochrome' model for microbe-to-mineral
358   electron transfer. *Mol Microbiol* **85**: 201-212.
359   Shi L, Rosso KM, Clarke TA, Richardson DJ, Zachara JM & Fredrickson JK (2012) Molecular Underpinnings
360   of Fe(III) Oxide Reduction by Shewanella Oneidensis MR-1. *Front Microbiol* **3**: 50.
361   Simon J (2002) Enzymology and bioenergetics of respiratory nitrite ammonification. *FEMS Microbiol Rev* **26**:
362   285-309.
363   Simpson PJ, Richardson DJ & Codd R (2010) The periplasmic nitrate reductase in Shewanella: the resolution,
364   distribution and functional implications of two NAP isoforms, NapEDABC and NapDAGHB. *Microbiology*
365   **156**: 302-312.
366   Tang YJ, Meadows AL, Kirby J & Keasling JD (2007) Anaerobic central metabolic pathways in Shewanella
367   oneidensis MR-1 reinterpreted in the light of isotopic metabolite labeling. *J Bacteriol* **189**: 894-901.
368   van Heeswijk WC, Westerhoff HV & Boogerd FC (2013) Nitrogen assimilation in Escherichia coli: putting
369   molecular data into a systems perspective. *Microbiol Mol Biol Rev* **77**: 628-695.
370   Wang H & Gunsalus RP (2003) Coordinate regulation of the Escherichia coli formate dehydrogenase fdnGHI
371   and fdhF genes in response to nitrate, nitrite, and formate: roles for NarL and NarP. *J Bacteriol* **185**: 5076-5085.
372   White GF, Edwards MJ, Gomez-Perez L, Richardson DJ, Butt JN & Clarke TA (2016) Mechanisms of Bacterial
373   Extracellular Electron Exchange. *Adv Microb Physiol* **68**: 87-138.
374   Wilkinson JF (1963) Carbon and energy storage in bacteria. *J Gen Microbiol* **32**: 171-176.

375
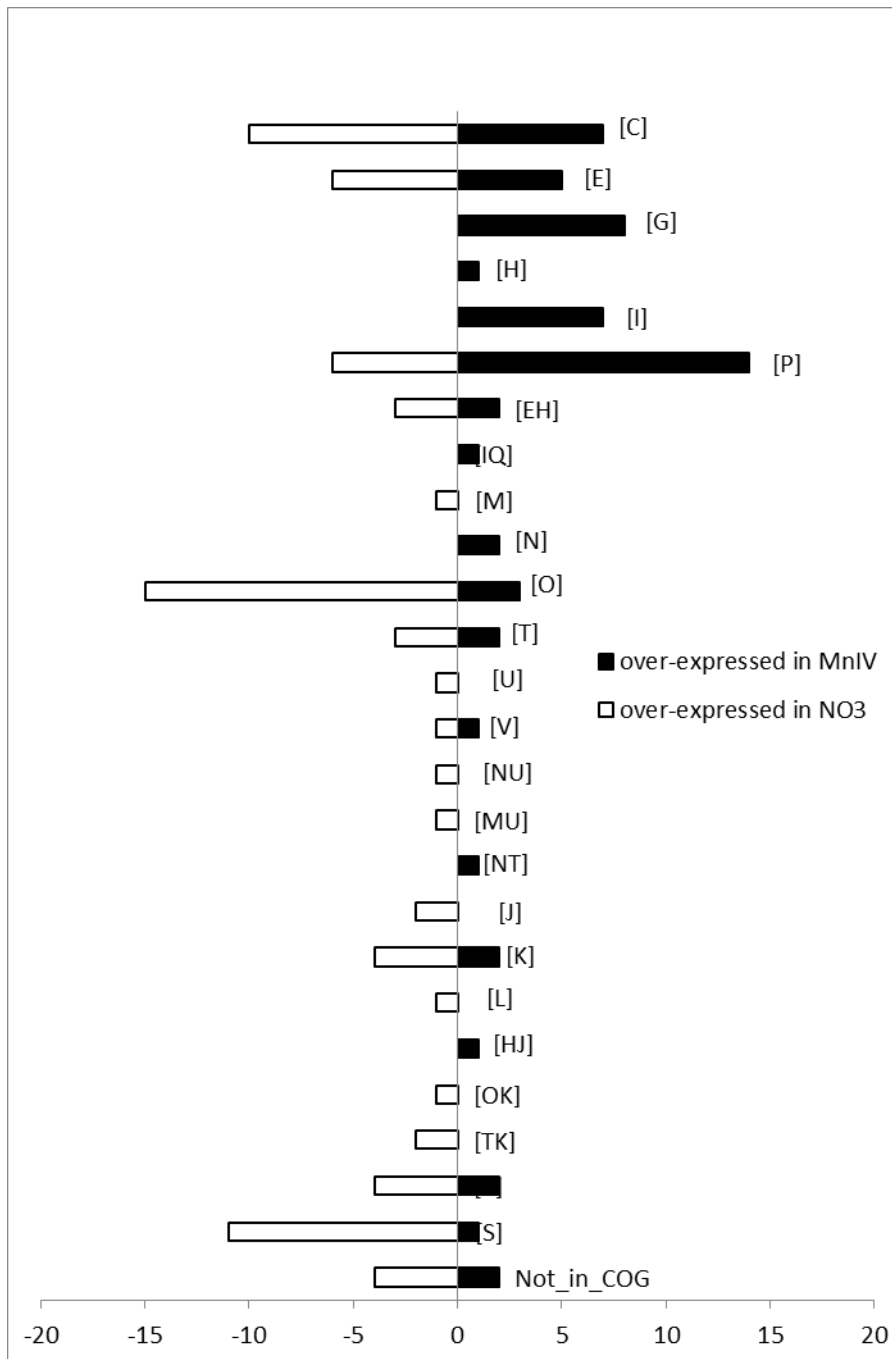
Fig.1. Over-expressed genes in manganese oxide or nitrate condition based on genes belonging to a COG categories (adjusted p-value <0.05). C, energy production and conversion; E, amino acid transport and metabolism; F, nucleotide transport and metabolism; G, carbohydrate transport and metabolism; H, coenzyme metabolism; I, lipid metabolism; J, translation, ribosomal structure, and biogenesis; K, transcription; L, DNA replication, recombination, and repair; M, cell envelope biogenesis, outer membrane; N, cell motility and secretion; O, posttranslational modification, protein turnover, and chaperones; P, inorganic ion transport and metabolism; Q, secondary metabolite biosynthesis, transport, and catabolism; R, general function prediction only; S, function unknown; T, signal transduction mechanisms; V, defense mechanisms
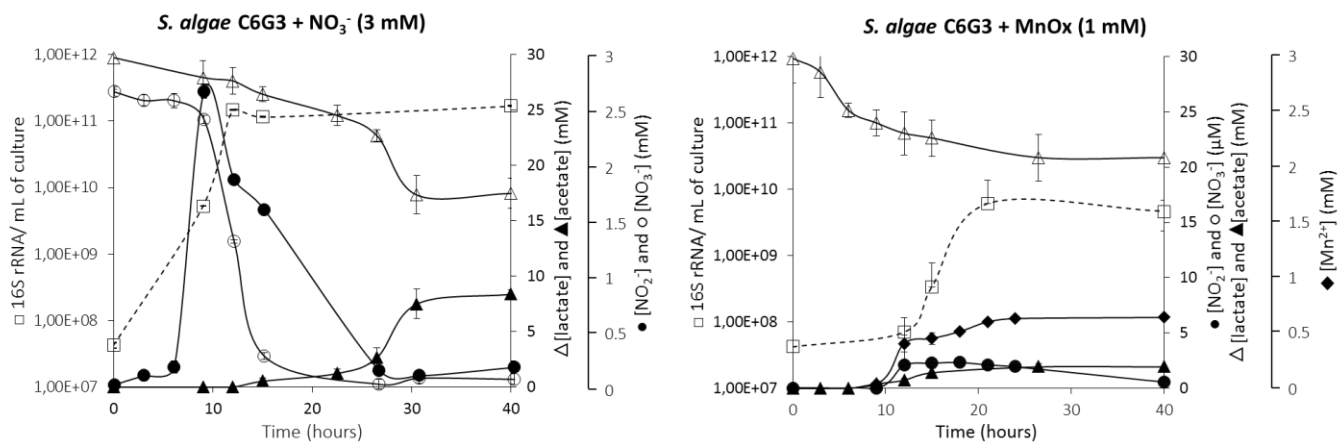
Fig. 2: Kinetic of growth of *S. algae* C6G3 in anaerobiosis and in the presence of nitrate or Mn(IV) as electron acceptor in minimal medium with lactate as electron donor. Bars represent the standard deviation.
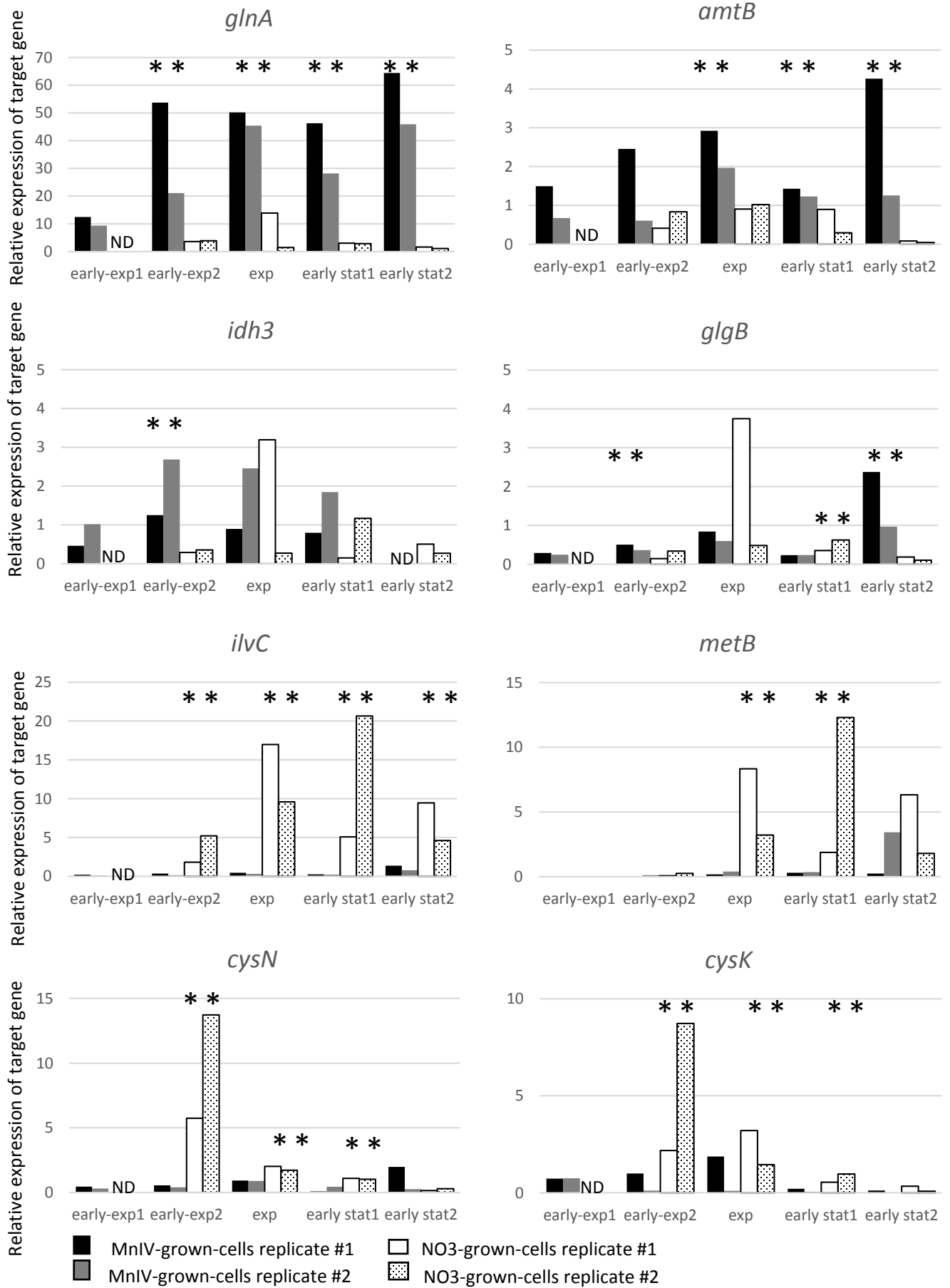
Fig.3. Gene expression level relative to *rpoD* of ammonium, sulfate assimilation and aa synthesis pathway along anaerobic bacterial growth with nitrate or manganese-oxide as the electron acceptor. *amtB*: ammonium transporteur, *glnA:* glutamine synthesis, *IDH:* 2 oxoglutarate synthesis, *cysN*: sulfate assimilation pathway , *cysK*: cystein synthesis, *ilC*: valine synthesis pathway , *metB*: methionine synthesis. *denotes difference in expression level between condition. ND: Not determined
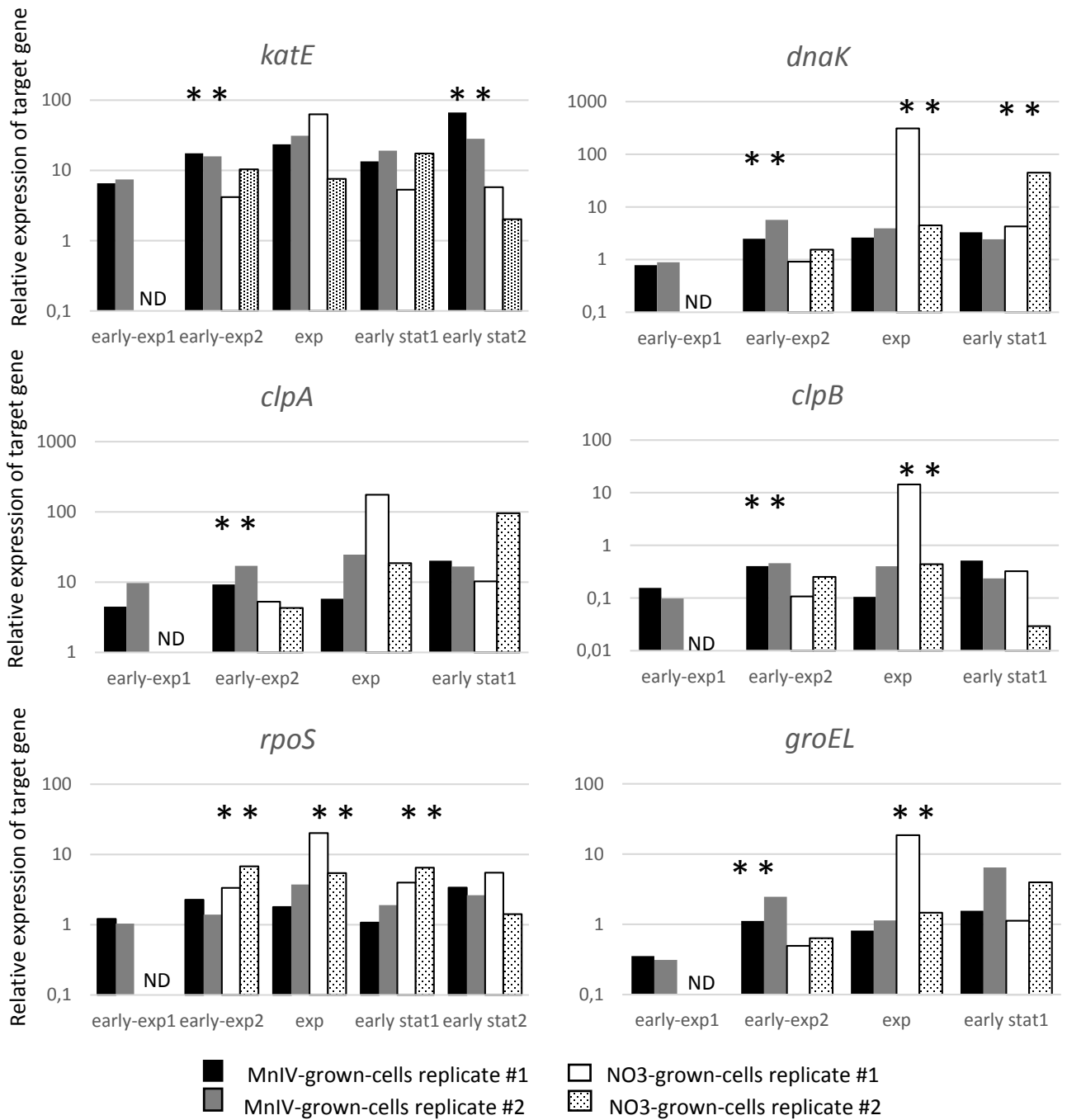
Fig.4. Genes of stress response. Expression level relative to *rpoD*
ATP-dependent Clp protease ATP-binding subunit *clpA*; katalase, *katE*; chaperonin GroEL,
groEL , chaperone protein DnaK, *dnaK*.; * denotes difference in expression level between
conditions. ND: Not determined.

The nature of electron acceptor (MnIV/NO3) triggers differential expression of genes associated with stress and ammonium limitation responses in *Shewanella algae* C6G3

Axel Aigle, Patricia Bonin, Nicolas Fernandez -Nunez , Béatrice Loriod, Sophie Guasco, Aurélie Bergon, Fabrice Armougom, Chantal Iobbi-Nivol, Jean Imbert, Valérie Michotey.

Table S1. Target gene characteristics: primer sequence, fragment size, annealing temperature (Tm) and references.

Primer	Target gene	Primer sequence (5' → 3')	Tm	Fragment size	Ref.
rpoD-F rpoD-R	*rpoD*	TAC GCC GAA GGC CTG AAA AT GAT AGA CAG GCC GGT TTC GG	62 °C	90 pb	Aigle et al 2017
cysK-F cysK-R	*cysK*	AGG CCT GTT GAC CAA AGA CA TCA ACT TGT AAC CTC GGG CG	62 °C	98 pb	This study
katE-F katE-R	*katE*	TGC AGG AGA GGT TGA TGC AG TGA AGG GTC CAG CAA GGG AT	62 °C	98 pb	This study
glgB-F glgB-R	*glgB*	GCC GAA CTC TTG GTG CCT TA GTT GAT AGC CCC AGG AAC CG	62 °C	100 pb	This study
glnA-F glnA-R	*glnA*	ACA GCC ACC TTT ATG CCC AA GCA AAT AGG TTG GTG CCG TC	62 °C	95 pb	This study
amt-F amt-R	*amt*	GCC AGG TTA ACC CTA TCC CG AGA ACC ACC GTT GAA ACC GA	62 °C	95 pb	This study
cysN-F cysN-R	*cysN*	TTG GTA TCA GGG CGA AAC CC CTG ACA TAC TGC ACC GGG AA	62 °C	99 pb	This study
dnaK-F dnaK-R	*dnaK*	TCT TTG GTG ATC AGT GGG GC CAC TGG CTCA CCC AGG AAA T	62 °C	101pb	This study
groEL-F groEL-R	*groEL*	GGG CGT GAA TGT TCT GGC TA TCT TTG GTG ATC AGT GGG GC	62 °C	102pb	This study
katE-F katE-R	*katE*	TGC AGG AGA GGT TGAT GCA G TGA AGG GTC CAG CAA GGG A	62 °C	98bp	This study
IDH3-F IDH3-R	*IDH3*	GAA AGT GGC CCG TGA AGT C GTT TTC CGG GTT CAT CAC CA	60 °C	100pb	This study
clpA-F clpA-R	*clpA*	AAG GTG GAC ATT CAC GAG CC GGG TGT AAC GCA CTC CAT GA	62 °C	97pb	This study
clpB-F clpB-R	*clpB*	ATC CTA ACC GGC CCA TAG GT GTG TCG AAC AGG AAC TTG GC	62 °C	97pb	This study
metB-F metB-R	*metB*	GCC GTG ATT GCC AAA GAT CC GGT CAG GTA GCT GTC GAA GG	62 °C	96 pb	This study
ilvC-F ilvC-R	*ilvC*	AAT GGC GAC GGT TTG GAG AT CCG ACT TCA CCT CGG CAA TA	62 °C	100 pb	This study

Table S2: Absolute quantification of cDNAs of interest per ng of RNA added in the reverse transcription reactions, in early (1 and 2) exponential, and stationary (1 and 2) phases of growth of S algae grown with nitrate or MnIV as electron acceptor. Value for the 2 independent cultures for each condition (MnIV or NO3) are shown

	early-exp1	early-exp2	exp	early stat1	early stat2		median value for both duplicate
rpoD-1-ngARN-Mn	6495.24	2299.51	1458.86	7076.27	220.59		1486.81
rpoD-2-ng ARN-Mn	3904.23	1335.19	743.75	1773.24	1514.76		
rpoD-1-ngARN-NO3	ND	25336.46	377.95	15699.54	5370.15		5474.30
rpoD-2-ng ARN-NO3	ND	5578.45	4790.86	1038.03	8301.43		
katE1-1-ngARN-Mn	42584.54	40288.33	34284.51	95172.72	14713.48		34081.89
KatE-2-ng ARN-Mn	29005.44	21205.85	23227.09	33879.27	42714.03		
katE1-1-ngARN-NO3	ND	105862.42	23758.27	83339.97	30979.72		33645.37
KatE-2-ng ARN-NO3	ND	57859.39	36311.02	18090.86	16750.27		
glgB-1-ngARN-Mn	1869.37	1154.82	1229.40	1653.14	523.79		839.30
glgB-2-ng ARN-Mn	952.20	483.14	443.34	416.63	1463.71		
glgB1-ngARN-NO3	ND	3631.94	1417.17	5511.62	988.66		1646.86
glgB-2-ng ARN-NO3	ND	1876.54	2305.59	645.63	856.25		
glnA-1-ngARN-Mn	81049.66	123506.96	73248.25	327575.89	14213.05		59791.98
glnA-2-ng ARN-Mn	36466.36	28197.21	33794.79	50007.44	69576.51		
glnA-1-ngARN-NO3	ND	91628.78	5255.36	47389.23	8812.69		8978.83
glnA-2-ng ARN-NO3	ND	21747.11	6993.46	2998.06	9144.97		
ilvC-1-ngARN-Mn	1333.69	826.75	678.82	1753.44	301.10		540.71
ilvC2-ng ARN-Mn	424.56	207.25	236.58	402.60	1176.47		
ilvC1-ngARN-NO3	ND	46246.53	6414.42	79707.23	50777.09		42142.48
ilvC-2-ng ARN-NO3	ND	29050.54	45975.55	21439.82	38309.41		
phoP-1-ngARN-Mn	11049.49	9601.85	5378.20	11879.61	877.62		6855.89
phoP-2-ng ARN-Mn	9094.41	5746.03	5477.82	7965.75	14321.55		
phoP-ngARN-NO3	ND	10050.80	4335.99	18318.20	22126.69		8966.92
phoP-2-ng ARN-NO3	ND	5716.98	9061.74	8005.89	8872.09		
ropS-1-ngARN-Mn	7834.70	5211.83	2601.29	7562.23	743.03		3074.26
ropS-2-ng ARN-Mn	4050.40	1854.12	2773.34	3375.17	3986.71		
ropS-1-ngARN-NO3	ND	84787.33	7623.34	62474.59	29503.58		27731.14
ropS-2-ng ARN-NO3	ND	37827.97	25958.70	6715.20	11727.45		
amtB-1-ngARN-Mn	9700.06	5644.67	4260.78	10124.17	940.87		2042.34
amtB-2-ng ARN-Mn	2632.72	811.34	1463.54	2180.80	1903.89		
amtB-1-ngARN-NO3	ND	10415.35	342.36	14083.75	434.93		2546.16
amtB-2-ng ARN-NO3	ND	4657.40	4886.43	303.82	372.74		
cysK-1-ngARN-Mn	4755.36	2292.21	2730.06	1491.15	27.45		128.43
cysK-2-ng ARN-Mn	2929.67	158.14	79.44	98.71	0.00		
cysK-1-ngARN-NO3	ND	55302.10	1213.15	8587.36	1829.35		4399.44

cysK-2-ng ARN-NO3	ND	48680.86	6969.53	1008.51	685.09		
cysN-1-ngARN-Mn	2968.42	1269.33	1341.75	581.76	436.18		622.88
cysN-2-ng ARN-Mn	1197.14	541.64	664.01	798.02	392.81		
cysN-1-ngARN-NO3	ND	145449.12	762.61	17252.64	836.04		5339.74
cysN-2-ng ARN-NO3	ND	76586.95	8237.84	1063.39	2441.64		
impG-1-ngARN-Mn	2887.61	468.74	266.81	831.90	129.82		129.06
impG-2-ng ARN-Mn	923.80	128.31	67.08	117.67	118.80		
impG-1-ngARN-NO3	ND	4091.03	327.16	467.03	185.81		264.18
impG-2-ng ARN-NO3	ND	2022.83	136.06	201.20	91.28		
metB-1-ngARN-Mn	39.54	111.58	262.75	2143.65	53.48		279.38
metB-2-ng ARN-Mn	41.13	161.79	296.01	632.11	5204.83		
metB-1-ngARN-NO3	ND	1743.54	3151.11	29435.18	33988.97		13859.03
metB-2-ng ARN-NO3	ND	1426.87	15428.42	12767.69	14950.37		
aceA-1-ng ARN-Mn	404.67	335.09	365.81	529.71			437.08
aceA-2-ng ARN-Mn	1841.14	501.77	499.46	374.71			
aceA-1-ng ARN-NO3	ND	14060.91	528.61	9030.90	7836.71		2653.92
aceA-2-ng ARN-NO3	ND	3162.80	2145.04	1016.46	1035.42		
aceB-1-ng ARN-Mn	15.22	4.01	7.66	8.14	ND		7.90
aceB-2-ng ARN-Mn	46.05	0.00	10.34	8.78	ND		
aceB-1-ng ARN-NO3	ND	320.46	102.63	0.00	205.21		102.21
aceB-2-ng ARN-NO3	ND	101.79	144.74	0.00	57.12		
clpA-1-ng ARN-Mn	29156.47	21295.70	8491.87	143010.12	ND		22054.73
clpA-2-ng ARN-Mn	37951.11	22813.76	18346.82	29660.86	ND		
clpA-1-ng ARN-NO3	ND	133583.58	66358.74	161244.98	269627.47		116544.63
clpA-2-ng ARN-NO3	ND	24002.63	89376.14	99505.68	162236.66		
clpB-1-ng ARN-Mn	1011.61	928.19	153.06	3645.04	ND		516.07
clpB-2-ng ARN-Mn	382.51	612.56	298.30	419.58	ND		
clpB-1-ng ARN-NO3	ND	2724.05	5430.77	5062.44	5151.05		3893.24
clpB-2-ng ARN-NO3	ND	1404.70	2104.60	30.41	9947.10		
dnaK-1-ng ARN-Mn	5108.80	5723.75	3815.04	23368.02	ND		5020.10
dnaK-2-ng ARN-Mn	3481.55	7568.59	2916.27	4316.46	ND		
dnaK-1-ng ARN-NO3	ND	23202.46	116840.11	67171.24	162488.17		56752.60
dnaK-2-ng ARN-NO3	ND	8632.92	21428.57	46333.96	221854.30		
IDH3-1-ng ARN-Mn	2994.22	2876.79	1306.72	5645.21	ND		3075.27
IDH3-2-ng ARN-Mn	3971.72	3587.42	1827.55	3273.74	ND		
IDH3-1-ng ARN-NO3	ND	7361.28	1206.87	2328.58	2710.93		2101.60
IDH3-2-ng ARN-NO3	ND	1970.10	1301.59	1212.98	2233.09		
groEL-1-ng ARN-Mn	2293.31	2564.04	1184.43	11006.34	ND		2926.32
groEL-2-ng ARN-Mn	1213.05	3288.60	842.86	11436.53	ND		
groEL-1-ng ARN-NO3	ND	12510.74	7024.71	17601.16	8583.02		7803.86
groEL-2-ng ARN-NO3	ND	3529.53	7011.11	4100.57	31333.75		

Table S3. Summary statistics of RNA-seq runs

TGML_ID	Sample_ID	Bases	≥ Q20	Reads	Reads Mapped	% Mapping
581	NO3_1_C6G3	63,727,883	55,673,431	469,736	390,727	83.18
582	NO3_2_C6G3	81,989,316	72,118,405	563,025	509,908	90.57
583	MnOx_1_ C6G3	58,840,970	51,594,018	411,316	384,501	93.48
584	MnOx_2_ C6G3	26,980,852	24,279,815	281,007	267,923	95.34

Table S4. List of differentially expressed genes under MnOx conditions as NO$_3^-$ with an adjusted p-value <0.05. The genes discussed in the article are indicated in bold.

Locus_tag JGI SA002_	Product_name	Code COG	COG	KEEG Orthology	E.C. number	Log2 fold change MnOx vs. NO3-
00257	**Malate synthase, aceB, glcB**	**C**	**2225**	**K01638**	**2.3.3.9**	**3.50**
00704	Sodium pump decarboxylases, oadG (TC:3.B.1)	C	3630	K01573	4.1.1.3	2.97
00705	Oxaloacetate decarboxylase, oadA (00705+00706)	C	5016	K01571	4.1.1.3	2.40 2.99
00708	Sodium ion-translocating decarboxylase, oadB (TC:3.B.1)	C	1883	K01572	4.1.1.3	3.14
05135	**Anaerobic dehydrogenases, fdhA (TC:5.A.3)**	**C**	**0243**	**K00123**	**1.2.1.2**	**1.74**
05137	**Formate dehydrogenase, fdhC**	**C**	**2864**	**K00127**	**1.2.1.2**	**2.33**
00475	L-lactate dehydrogenase, lldE	C	2048	K18928		-1.67
03282	Acetate kinase, ackA	C	0282	K00925	2.7.2.1	-1.92
03376	**Formate dehydrogenase, nitrate inducible, fdnG (TC:5.A.3) (03376+03377+03378)**	**C**	**0243**	**K00123**	**1.2.1.2**	**-2.83 -3.19 -3.40**
03379	**Formate dehydrogenase fdnH**	**C**	**0437**	**K00124**		**-3.70**
03380	**Formate dehydrogenase, fdnI**	**C**	**2864**	**K00127**		**-4.25**
03386	**Formate dehydrogenase, fdhD**	**C**	**1526**	**K02379**		**-6.11**
05459	**Formate dehydrogenase, fdoI**	**C**	**2864**	**K00127**		**-5.63**
05460	**Formate dehydrogenase, fdoH**	**C**	**0437**	**K00124**		**-4.21**
05461	**Formate dehydrogenase, fdoG, fdfH (05461+05462) (TC :5.A.3)**	**C**	**0243**	**K00123**	**1.2.1.2**	**-3.62**
02930	**Glutamine synthetase type I, glnA**	**E**	**0174**	**K01915**	**6.3.1.2**	**2.68**
04432	**Nitrogen regulatory protein P-II family, glnK**	**E**	**0347**	**K04752**		**5.52**
03298	**Cysteine synthase A, cysK**	**E**	**0031**	**K01738**	**2.5.1.47**	**2.55**
02212	**Sulfate adenylyltransferase, cysD**	**EH**	**0175**	**K00957**	**2.7.7.4**	**3.72**
02218	**Phosphoadenylyl-sulfate reductase thioredoxin-dependent, cysH**	**EH**	**0175**	**K00390**	**1.8.4.8**	**3.86**
05500	**Asparagine synthase, asnB**	**E**	**0367**	**K01953**	**6.3.5.4**	**6.57**

03348	**Cystathionine gamma-synthase, metB**	**E**	**0626**	**K01739**	**2.5.1.48**	**-3.21**
03349	**Aspartate kinase, metL**	**E**	**0527**	**K12525**	**1.1.1.3**	**-3.75**
03351	**5,10-methylenetetrahydrofolate reductase (NAD(P)), metF**	**E**	**0685**	**K00297**	**1.5.1.20**	**-3.83**
05416	**5-methyltetrahydrofolate--homocysteine methyltransferase, metH (05414+05415+05416+05417)**	**E**	**1410**	**K00548**	**2.1.1.13**	**-3.53**
03382	Selenocysteine synthase, selA (3382+3383)	E	1921	K01042	2.9.1.1	-5.14 -2.85
03737	Aspartate kinase, thrA	E	0527	K12524	1.1.1.3	1.89
02783	**Ketol-acid reductoisomerase, ilvC (02783+02784)**	**EH**	**0059**	**K00053**	**1.1.1.86**	**-3.93 -4.59**
04508	**Acetolactate synthase, ilvB, ilvG, ilvI**	**EH**	**0028**	**K01652**	**2.2.1.6**	**-1.99**
01676	6-phosphogluconolactonase, pgl (01676+01677)	G	0363	K01057	3.1.1.31	2.38
01732	**4-alpha-glucanotransferase, malQ 01732+01733**	**G**	**1640**	**K01196**	**2.4.1.25**	**5.54 4.75**
01734	**Alpha-1,4-glucan:alpha-1,4-glucan 6-glycosyltransferase, glgB**	**G**	**0296**	**K00700**	**2.4.1.18**	**4.23**
01735	**Glycogen debranching enzyme**	**G**	**1523**	**K01196**	**3.2.1.33**	**3.66**
01738	**Glycogen/starch/alpha-glucan phosphorylases, glgP**	**G**	**0058**	**K00688**	**2.4.1.1**	**2.65**
01739	**Glucose-1-phosphate adenylyltransferase, glgC**	**G**	**0448**	**K00975**	**2.7.7.27**	**3.22**
01742	**Glycogen synthase, glgA**	**G**	**0297**	**K00703**	**2.4.1.21**	**2.49**
02214	Uroporphyrinogen-III C-methyltransferase, cobA (02213+02214)	H	0007	K02303	2.1.1.107	4.04
02545	Alpha-L-glutamate ligases, rimK	HJ	0189	K05844	6.3.2.-	4.58
00520	**Acyl-CoA hydrolase**	**I**	**1607**	**K01073**	**3.1.2.20**	**4.40**
01239	**Acyl-CoA dehydrogenases, fadE**	**I**	**1960**	**K06445**	**1.3.99.2**	**2.32**
01583	**Acetyl-CoA dehydrogenase, fadE (01583+1584)**	**I**	**1960**	**K06445**	**1.3.99.3**	**2.06 1.81**
05346	**3-hydroxyacyl-CoA dehydrogenase, fadB**	**I**	**1250**	**K01825**	**4.2.1.17/ 5.3.3.8**	**1.77**
05347	**Fatty oxidation complex, beta subunit, fadA (05347+05348+05349)**	**I**	**0183**	**K00632**	**2.3.1.16**	**2.03 2.58**
04827	Acyl-CoA synthetases (TC:4.C.1), fadD	IQ	0318	K01897	6.2.1.3	1.80
03384	Selenocysteine-specific elongation factor, selB	J	3276			-4.25
05662	LSU ribosomal protein L29P, rpmC	J	0255	K02904		-2.00
04899	'Cold-shock' DNA-binding domain, cspA	K	1278	K03704		3.07
04948	**RNA polymerase, sigma 38 subunit, rpoS**	**K**	**0568**			**1.94**
00591	Zn(II)-responsive transcriptional regulator, zntR	K	0789	K13638		-3.55
01336	Transcriptional regulator, MarR family	K	1846			-3.32
01904	Transcriptional regulator, LysR family, metR	K	0583	K03576		-2.70
03691	Transcriptional regulator, LysR family, nhaR	K	0583	K03717		-1.97
00380	AAA domain, sbcC	L	0419	K03546		-2.28
02357	Outer membrane protein (porin)	M	3203			-1.84
02631	Outer membrane protein TolC, TC:1.B.17	MU	1538			-4.46

00350	Flagellin FlaG, flaG	N	1334	K06603		1.92
00351	Flagellin, fliC	N	1344	K02406		2.22
00148	Methyl-accepting chemotaxis protein, mcp	NT	0840	K03406		2.83
00338	Flagellar biosynthesis/type III secretory pathway protein, fliH (TC:3.A.6)	NU	1317	K02411		-1.91
00485	Membrane-bound serine protease, nfeD (00483+00484+00485)	O	1030	K07403		4.90
00748	Subtilisin-like serine proteases	O	1404			3.88
04897	**ATP-dependent Clp protease ATP-binding subunit ClpA, clpA**	**O**	**0542**	**K03694**	**3.4.21.92**	**1.59**
00037	lon ATP-dependent Lon protease 00036+00037	O	0466	K01338	3.4.21.53	-2.03
00466	Molecular chaperone GrpE (heat shock protein), grpE	O	0576	K03687		-1.85
00886	Molecular chaperone, HSP90, htpG (00886+00887)	O	0326	K04079		-2.86
01859	**ATP-dependent Clp protease, clpB (01858+01859)**	**O**	**0542**	**K03695**		**-2.58**
01989	Subtilisin-like serine proteases (01989+01990+01991)	O	1404			-3.37
02096	GlyGly-CTERM domain (serine protease) (02096+02097+02098)	O	1404			-2.99
02252	AAA domain (Cdc48 subfamily), protein VasG (TC:3.A.23.1)	O	0542	K11907		-4.77
02658	Threonine peptidase, hslV	O	5405	K01419	3.4.25.2	-2.86
02659	ATP-dependent protease HslVU, hslU	O	1220	K03667		-2.13
03381	Formate dehydrogenase accessory protein, fdhE	O	3058	K02380		-4.11
03391	Predicted redox protein, regulator of disulfide bond formation	O	0425			-5.55
03418	**Chaperonin GroEL, groEL**	**O**	**0459**	**K04077**		**-3.07**
04171	**Chaperone protein DnaK, dnaK (TC:1.A.33)**	**O**	**0443**	**K04043**		**-2.73**
04497	Molecular chaperone, ibpA 04497+04498	O	0071	K04080		-3.13
05458	Formate dehydrogenase maturation protein, fdhE	O	3058	K02380		-5.82
01619	Hydrogenase accessory protein HypB (01619+01620)	OK	0387	K04652		-3.89
01044	TonB dependent receptor/TonB-dependent Receptor Plug Domain (TC:1.B.14)	P	1629	K02014		2.34
02205	**Adenylylsulfate kinase, cysC**	**P**	**0529**	**K00860**	**2.7.1.25**	**2.41**
02208	Di- and tricarboxylate transporters (TC:2.A.47) (02206+02207+02208)	P	0471			4.20 3.18
02209	**Sulfate adenylyltransferase, cysN**	**P**	**2895**	**K00956**	**2.7.7.4**	**4.32**
02219	**Nitrite/Sulfite reductase, cysI (02219+02220+02221)**	**P**	**0369**	**K00381**	**1.8.1.2**	**6.07 4.97 4.30**
02222	**Sulfite reductase (NADPH), cysJ**	**P**	**0369**	**K00380**	**1.8.1.2**	**5.60**
02606	TonB dependent receptor (TC:1.B.14) (02605+02606)	P	4771	K02014		2.69 3.01
03501	**Catalase (03500+03501), katE**	**P**	**0753**	**K03781**	**1.11.1.6**	**4.86 4.56**

03616	Bacterioferritin, bfr	P	2193	K03594		2.12
04433	**Ammonium transporter, amtB (TC:1.A.11)**	**P**	**0004**	**K03320**		**6.09**
01335	Cation diffusion facilitator family transporter (TC:2.A.4)	P	1230			-3.64
03292	Outer membrane receptor proteins, mostly Fe transport (TonB) (TC:1.B.14)	P	1629	K02014		-2.41
03997	ATPase, P-type (transporting), HAD superfamily, subfamily IC/heavy metal translocating P-type ATPase (TC:3.A.3) (03996+03997+03998)	P	2217	K01534	3.6.3.3/ 3.6.3.5	-3.45 -2.59
04430	**Respiratory nitrite reductase, nrfA**	**P**	**3303**	**K03385**	**1.7.2.2**	**-2.49**
04805	Outer membrane receptor proteins, mostly Fe transport (TonB) (TC:1.B.14)	P	1629	K02014		-2.29
02934	Predicted permease, DMT superfamily, pecM (TC:2.A.7)	R	5006	K15269		2.92
04332	Protein related to penicillin acylase, pvdQ (04329+04330+04331+04332)	R	2366	K07116		2.58
00592	Predicted permease (TC:9.B.28), putative copper/zinc efflux protein	R	0701	K07089		-2.87
00730	Predicted esterase	R	0400			-1.75
01001	Extracellular nuclease, putative (01000+01001)	R	2374	K7004		-3.00
03387	Predicted transporter component	R	2391	K07112		-4.41
00506	Uncharacterized conserved protein	S	5507			3.15
00252	Uncharacterized protein conserved in bacteria	S	3228	K09933		-3.61
02247	Type VI secretion protein, icmF	S	3523	K11891		-3.34
02248	Type VI secretion-associated protein, impA	S	3515	K11910		-3.88
02255	Type VI secretion protein, impJ/vasE	S	3522	K11893		-3.29
02261	Type VI secretion protein, impG/vasA	S	3519	K11896		-4.17
02262	Type VI secretion system lysozyme-like protein	S	3518	K11905		-3.87
02263	Type VI secretion protein, impC	S	3517	K11900		-4.19
02264	Type VI secretion protein, impB	S	3516	K11901		-4.92
02704	Uncharacterized protein conserved in bacteria (02704+2705)	S	4582			-2.58
03311	Uncharacterized conserved protein (03311+03312)	S	2968	K09807		-2.99 -2.42
02939	**Signal transduction histidine kinase, nitrogen specific NRI, *ntrB/glnG***	**T**	**3852**	**K07708**	**2.7.13.3**	**2.93**
02940	**Nitrogen metabolism transcriptional regulator NRII, *ntrC/glnL***	**T**	**2204**	**K07712**		**3.51**
03696	Negative regulator of sigma E activity, rseA	T	3073	K03597		-2.07
03697	Sigma E regulatory protein, MucB/RseB, rseB (03697+03698)	T	3026	K03598		-2.15 -2.59
02250	Sigma-54 specific transcriptional regulator, vasH	TK	1221	K11908		-5.56
05562	Two component transcriptional regulator, winged helix family, phoP	TK	0745	K07660		-2.07
02258	FHA domain protein, impI, vasC	U	3456	K11894		3.68
00404	Cation/multidrug efflux pump (TC:2.A.6)	V	0841			3.29
02630	Multidrug resistance efflux pump	V	1566			-3.82

00070	Lysine-specific metallo-endopeptidase	K08646	3.4.24.20	2.97
02245	ImpA-related N-terminal, vasL (02245+02246)	K11911		-3.74
02249	Type VI secretion-associated protein, vasI (TC:3.A.23.1)	K11909		-4.31
03106	Conserved hypothetical protein 698 (TC:2.A.98)			2.82
03389	Sulphur transport (03389+03390)	K07112		-3.67
04527	TonB dependent receptor/TonB-dependent Receptor Plug Domain (TC:1.B.14)			-1.90
04506	OmpA family			2.07
05025	hypothetical protein			-2.00
00064	**decaheme c-type cytochrome, OmcA/MtrC family, mtrH**			**-1.90**
00068	**decaheme c-type cytochrome, DmsE family, mtrA**			**-2.44**
00378	hypothetical protein			-3.96
00475	Cysteine-rich domain			-1.67
00519	hypothetical protein			2.99
03974	Protein of unknown function (DUF1107)			-2.19
01871	hypothetical protein			-3.67
01993	Curlin associated repeat			-2.83
02089	hypothetical protein			-2.07
02232	hypothetical protein			1.99
02543	Conserved hypothetical protein 2001, proteobacterial 02543 +02544			5.77 5.25
02554	hypothetical protein			3.37
02555	N-linked glycosylation glycosyltransferase PglG			4.65
03104	Protein of unknown function (DUF3612)/Helix-turn-helix domain			2.07
05454	Ankyrin repeats (3 copies)			-1.87
04188	hypothetical protein			3.11
03150	Extracellular lipase, Pla-1/cef family 03150 + 03151			2.35 2.45
03389	Sulphur transport			-3.68
03502	Transposase			4.56
04332	Penicillin amidase			2.58

Table 5. Blastn *katE* (SA002_03500+SA002_03501) from *Shewanella algae* C6G3 against all *Shewanella* isolate available on JGI (n=62), and fitness BLAST significant results from JGI (Wetmore et al., 2015 and Rubin et al., 2015).

Genome name	Identities
Shewanella algae JCM 21037*	909/953 95%
Shewanella algae NBRC 103173*	909/953 95%

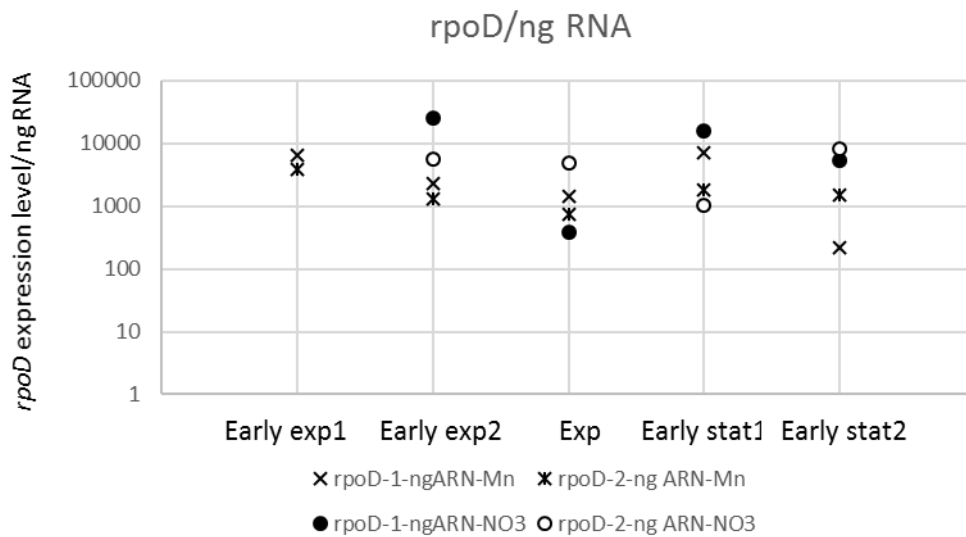| *Shewanella haliotis* JCM 14758*	908/953 95%
Shewanella sp. JCM 19057	907/953 95%
Shewanella sp. 38A_GOM-205m*	906/953 95%
Shewanella algae MARS 14*	905/953 95%
Shewanella sp. ECSMB14102	896/953 94%
Shewanella chilikensis JC5	878/953 92%
Shewanella algae ACDC*	864/951 91%

*synteny conserved

Fig S1. Absolute expression level of *rpoD* coding of the sigma 70 subunit of the RNA polymerase from duplicate cultures with either nitrate (round symbol) or manganese-oxide (cross symbol) as electron acceptor
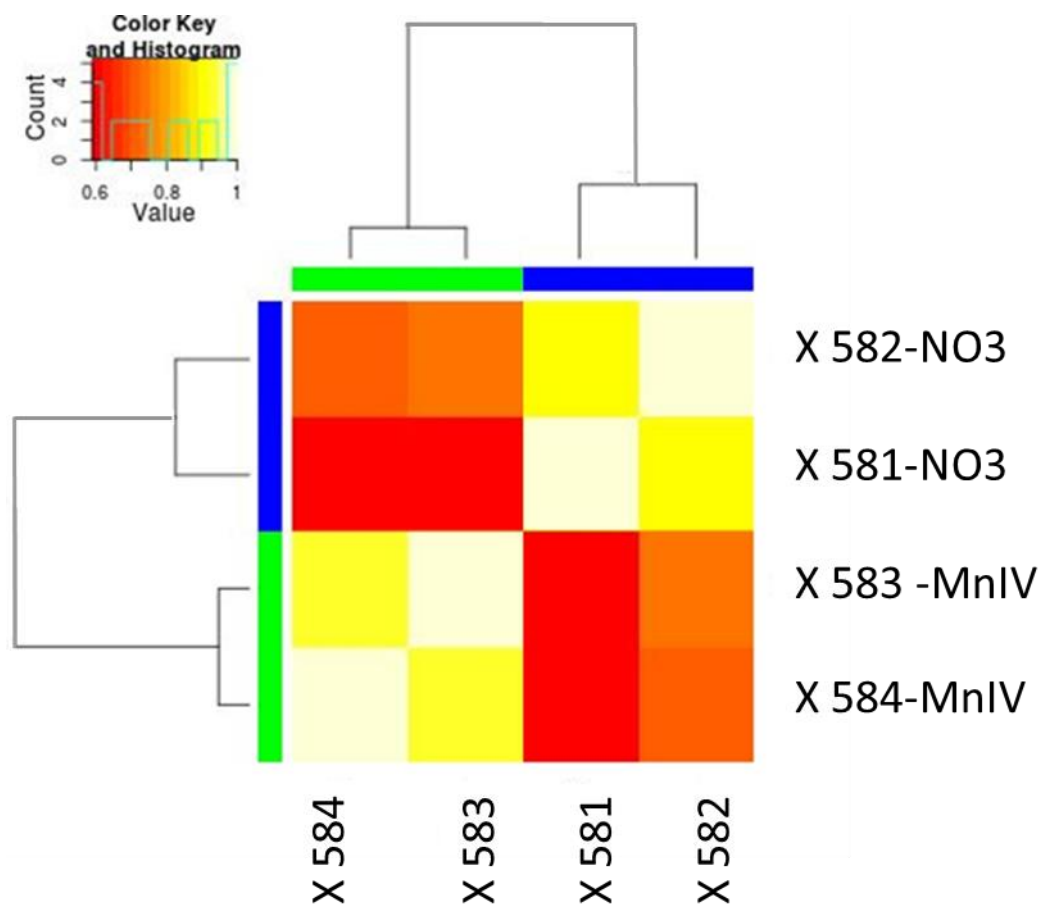
Fig S2. Correlation matrix between RNA-seq normalized expression levels of each independent culture obtained with DESeq.

The R package DESeq was used to analyze the differential expression of genes between the different culture conditions (Andres &Huber, 2010).

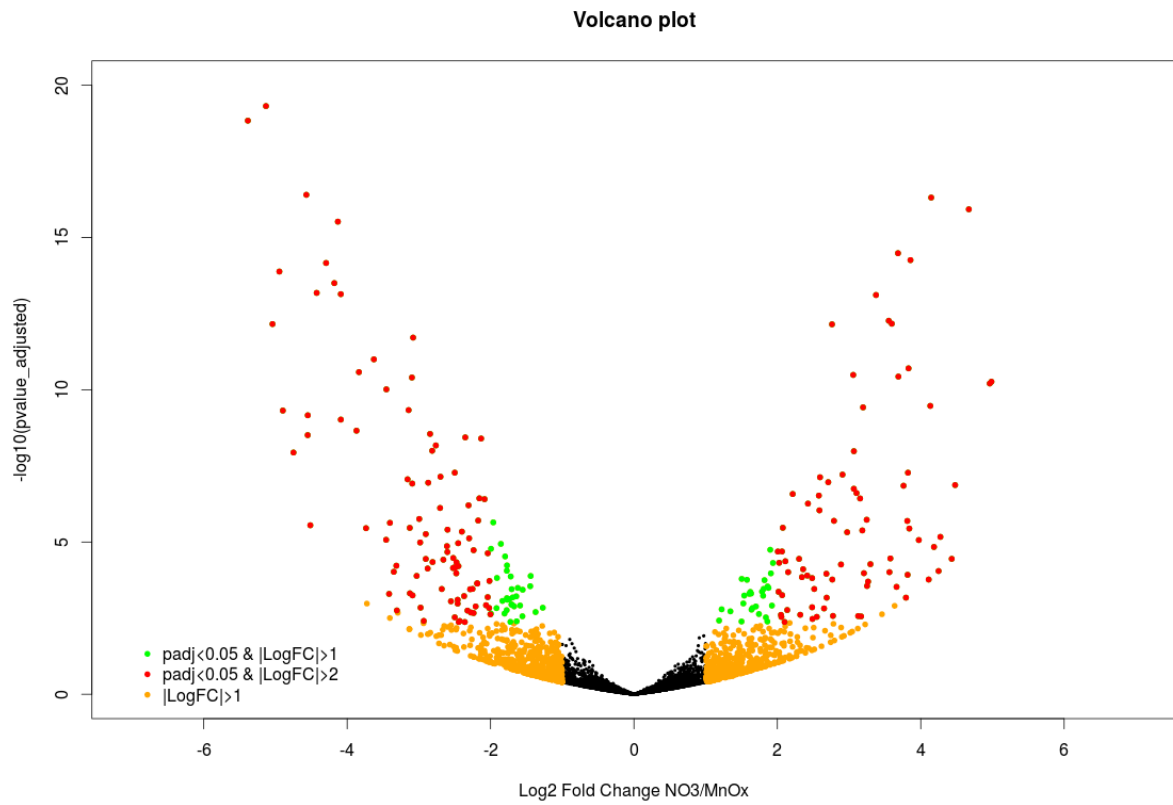Anders S, Huber W (2010) Differential expression analysis for sequence count data. Genome Biol 11: R106.

Figure S3. Volcano plot distribution showing transcriptomic data from S. algae C6G3 grown on nitrate (NO3-, right part) and manganese oxide (MnIV, left part) as electrons acceptors.
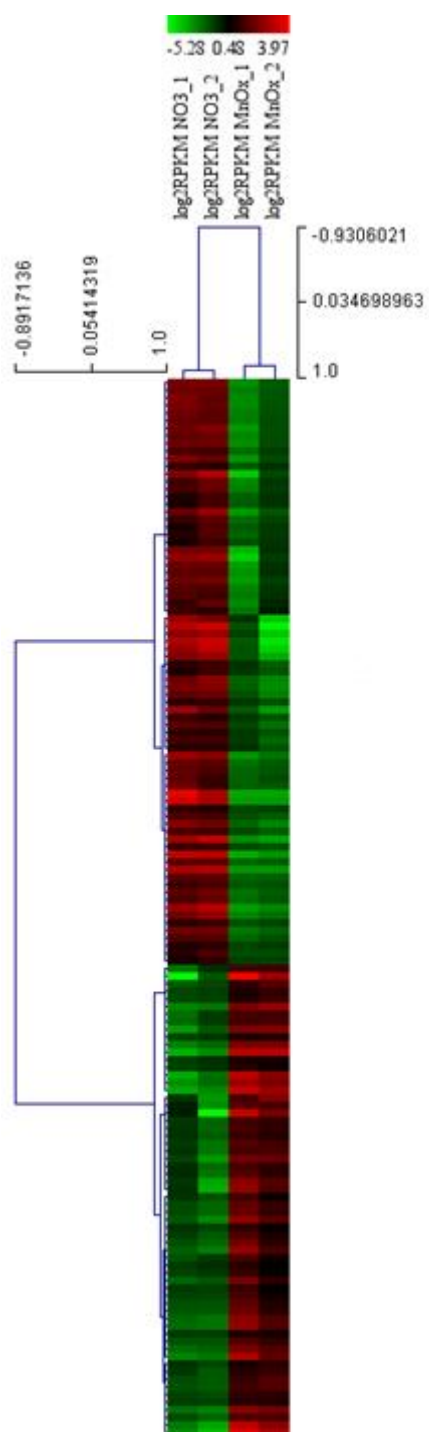
Fig S4: Heat mat of the log2 RPKM of overexpressed gene among the 4 independent cultures
(Two with nitrate as electron acceptor and 2 with MnIV as electron acceptor)

Material and methods

c-type cytochrome detection. Crude extracts (30 µg) of *S. algae* grown anaerobically in the presence of either fumarate, Mn or KNO3 were loaded on 12% SDS-PAGE. After migration, cytochromes were revealed by staining for peroxidase activity of hemes using 3,3',5,5'-tetramethylbenzidine (TMBZ)(Thomas et al 1976) .
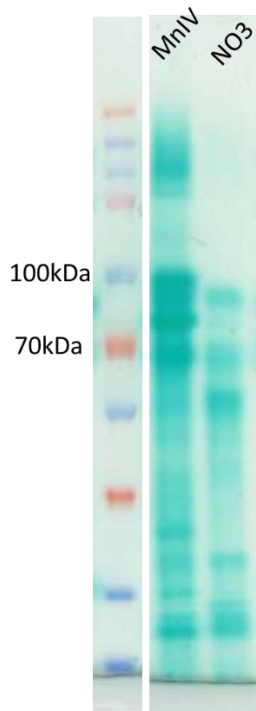

Fig S5. *c*-type cytochrome profile of *S. algae* according to the electron acceptor present in the growth medium.

Crude extract (30µg/µl) of cells grown in the presence of either fumarate, MnIV or NO3 were submitted to a 12% SDS-PAGE. After electrophoresis, *c*-type cytochromes were visualized by heme staining using TMBZ. M for MW markers

Thomas PE, Lu AY, Ryan D, West SB, Kawalek J, Levin W. Multiple forms of rat liver cytochrome P-450. Immunochemical evidence with antibody against cytochrome P-448. J Biol Chem 1976;251:1385–91.